

Flavor singlet axial vector coupling of the proton with dynamical Wilson fermions

S. Güsken,¹ P. Ueberholz,¹ J. Viehoff,² N. Eicker,² T. Lippert,¹ K. Schilling,^{1,2} A. Spitz,² and T. Struckmann¹

(SESAM Collaboration)

¹*Bergische Universität Wuppertal, Fachbereich Physik, 42097 Wuppertal, Germany*

²*NIC Forschungszentrum Jülich, and DESY, Hamburg, 52425 Jülich, Germany*

(Received 14 January 1999; published 27 April 1999)

We present the results of a full QCD lattice calculation of the flavor singlet axial vector coupling G_A^1 of the proton. The simulation has been carried out on a $16^3 \times 32$ lattice at $\beta=5.6$ with $n_f=2$ dynamical Wilson fermions. It turns out that the statistical quality of the connected contribution to G_A^1 is excellent, whereas the disconnected part is accessible but suffers from large statistical fluctuations. Using a 1st order tadpole improved renormalization constant Z_A , we estimate $G_A^1=0.20(12)$. [S0556-2821(99)04811-0]

PACS number(s): 12.38.Gc

I. INTRODUCTION

The flavor singlet axial vector coupling G_A^1 of the proton,

$$s_\mu G_A^1 = \langle P | \bar{u} \gamma_\mu \gamma_5 u + \bar{d} \gamma_\mu \gamma_5 d + \bar{s} \gamma_\mu \gamma_5 s | P \rangle, \quad (1)$$

where s_μ denotes the components of the proton polarization vector, has been the target of intensive research activity both in experimental and theoretical elementary particle physics over recent years. About one decade ago, the European Muon Collaboration (EMC) experiment found an unexpectedly small value, $G_A^1=0.12(17)$, from the measurement of the first moment of the spin dependent proton structure function g_p^1 in deep inelastic polarized muon-proton scattering [1]. Since G_A^1 can be interpreted in the naive parton model as the fraction of the proton spin carried by the quarks, the EMC result became known as the so called ‘‘proton spin crisis.’’

A number of succeeding experiments have been performed in the meantime [2–6]. The latest analysis [5], including proton, neutron, and deuteron data finds

$$G_A^1=0.29(6), \quad (2)$$

at a renormalization scale $\mu^2=5 \text{ GeV}^2$. This is still far away from the Ellis-Jaffe sum rule [7] expectation $G_A^1 \simeq G_A^8 = 0.579(25)$ [8], which is found in the Okubo-Zweig-Iizuka (OZI) limit of QCD.

As has been pointed out by Veneziano [9] a possible nontrivial topological structure of the QCD vacuum, which induces a nonzero contribution to the divergence of the axial vector flavor singlet current via the axial anomaly, might induce a sizeable effect on the value of the matrix element in Eq. (1). If one could prove that such vacuum effects indeed reduce the value of G_A^1 from 0.579 to 0.29, then, on the one hand, the ‘‘proton spin crisis’’ would be resolved since the naive parton interpretation and the OZI estimate of G_A^1 would be no longer valid. On the other hand, such a result would establish the existence of nontrivial topological vacuum structures, thus opening the door for a quantitative study of the connection between vacuum topology and instantons [10].

The lattice method provides an ideal tool to calculate the matrix element of Eq. (1) nonperturbatively. Within this method two complementary approaches have been developed over the recent years. The first is to evaluate the connected and disconnected contributions to the flavor singlet matrix element directly, which are schematically depicted in Fig. 1. This ‘‘direct method’’ will be dealt with in the present paper.

Alternatively, one can exploit the anomalous divergence equation of the flavor singlet axial vector current. Using this approach, the singlet coupling G_A^1 is extracted from the correlation function of the proton propagator and the topological charge density [11–13]. Although this ‘‘topological method’’ circumvents the computationally expensive calculation of disconnected (fermionic) contributions, it has some intrinsic difficulties. The connection between G_A^1 and the correlation of proton and topological charge density is valid in the limit of vanishing quark mass and zero momentum transfer only. As both these limits cannot be taken by a direct calculation on a finite lattice, two (wide range) extrapolations have to be performed. In addition, the ‘‘topological method’’ is ill defined in the quenched approximation of QCD [11]. On the other hand, the latter method provides the advantage of a nonperturbative renormalization procedure for the topological charge density [14,15].

The ‘‘direct method’’ has been tested on quenched configurations by Fukugita *et al.* [16] and Dong *et al.* [17] some time ago. Although the former study has been done at a somewhat strong coupling ($\beta=5.7$) and the latter is based on a very limited statistical sample (24 gauge configurations), the results are encouraging, as they find estimates for G_A^1 compatible with Eq. (2).

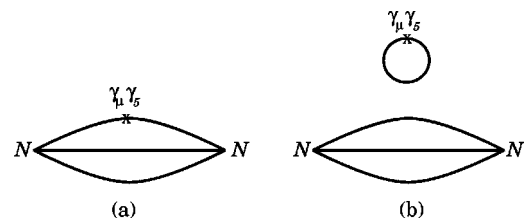


FIG. 1. Connected (a) and disconnected (b) contributions to the axial vector density amplitude of a nucleon. Please note that gluon lines connecting the quark lines are omitted.

It is of course by no means obvious, that these estimates hold also in full QCD. As we explained above, one expects vacuum contributions to lower the parton estimate of G_A^1 . The actual numbers might well depend on the details of the vacuum structure, such as the presence of sea quarks. Therefore, full QCD lattice simulations are necessary to calculate reliable QCD results for G_A^1 .

Exploratory full QCD studies using the ‘‘topological method’’ have been performed by the authors of Ref. [13] and Ref. [18], within the Kogut-Susskind lattice discretization scheme and with $n_f=4$ degenerate quark flavors. Both simulations suffer however from serious systematic uncertainties, as they have been performed at finite quark mass and sizeable momentum transfer [$q^2 \simeq (600 \text{ MeV})^2$].

In this paper we present the results of a full QCD calculation from the ‘‘direct method.’’

We have analyzed 200 gauge configurations at each of our four sea quark masses corresponding to $m_\pi/m_\rho = 0.833(3)$, $0.809(15)$, $0.758(11)$, and $0.686(11)$. The gauge configurations have been generated previously in the standard Wilson discretization scheme with $n_f=2$ mass degenerate quark flavors, at $\beta=5.6$ and with a lattice size of $n_s^3 \times n_t = 16^3 \times 32$ points. Details of the simulation can be found in Ref. [19].

As a preparing remark we emphasize that the numerical calculation of the disconnected parts of axial vector quantities is difficult, especially in full QCD simulations. It is known from lattice evaluations of the pion-nucleon-sigma term [20,21] that the signals for the disconnected contributions of scalar insertions suffer from large statistical fluctuations. Since the disconnected parts of axial vector quantities can be seen as the difference of two such scalar insertions, one can expect that the statistical noise is even more dangerous in the axial vector case. On top of this, a comparison between quenched and full QCD lattice results for the light spectrum revealed [19], that the statistical uncertainty in full QCD is larger by about a factor of 2 compared to a quenched calculation at equal statistics, cutoff, and lattice size. Thus, one major issue of this paper is to investigate whether and to what accuracy one can extract disconnected signals for axial vector quantities with state of the art methods and statistics in full QCD calculations.

The paper is organized as follows. In the next section we will briefly explain the methods used to calculate the connected and disconnected contributions to the matrix element of Eq. (1) and present our raw data. The chiral extrapolations and the renormalization are performed in Sec. III. A discussion of the physics results and concluding remarks are given in Sec. IV.

II. LATTICE METHODS AND RAW DATA

A. Connected contributions

To calculate the connected contributions to the axial vector density matrix element of the proton, Eq. (1), we have applied the global summation method [21,22]. With this technique one calculates the ratio

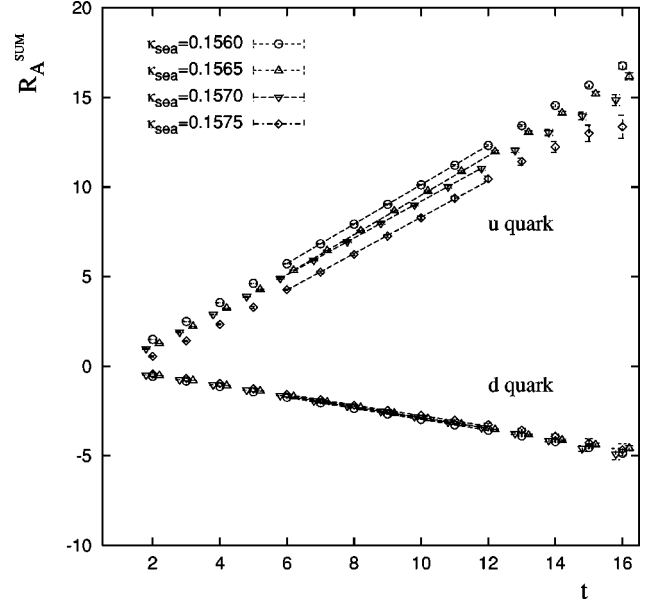


FIG. 2. Summation method: The raw data R_u and R_d for the spin averaged connected contributions at our sea quark masses. The fits (range and value) are indicated by dashed lines.

$$R_{A_\mu}^{SUM}(t) = \frac{\sum_x \left\langle P^\dagger(\vec{0},0) \sum_{y,y_0} [\bar{q} \gamma_\mu \gamma_5 q](\vec{y},y_0) P(\vec{x},t) \right\rangle}{\sum_x \langle P^\dagger(\vec{0},0) P(\vec{x},t) \rangle} - \left\langle \sum_{y,y_0} [\bar{q} \gamma_\mu \gamma_5 q](\vec{y},y_0) \right\rangle, \quad (3)$$

where P is an interpolating operator for the proton. From this ratio one extracts the matrix element $\langle P | \bar{q} \gamma_\mu \gamma_5 q | P \rangle$, which is given by the slope of the asymptotic form

$$R_{A_\mu}^{SUM}(t) \xrightarrow{t \rightarrow \infty} A + \langle N | \bar{q} \gamma_\mu \gamma_5 q | N \rangle t. \quad (4)$$

Note that there are two different types of connected insertions, one from the contraction of the ‘‘loop’’ quark q with the u -type quark of the proton and one from the contraction with the d -type quark. This yields

$$R_{q,\mu}(t) = A_q + C_{q,\mu} t,$$

$$C_{q,\mu} = \langle P(\kappa_{sea}) | [\bar{q} \gamma_\mu \gamma_5 q](\kappa_{sea}) | P(\kappa_{sea}) \rangle_{con}, \quad q = u, d. \quad (5)$$

The 3-point correlator in the numerator of Eq. (3) has been evaluated using the standard insertion technique [22]. To improve on the ground state projection of the proton we have applied ‘‘Wuppertal smearing’’ [23] with $n=50, \alpha=4$ to all proton operators.

In Fig. 2 we display the corresponding signals, spin averaged over $\gamma_\mu \gamma_5$, $\mu = 1, 2, 3$. The sea quark mass has been set

TABLE I. Lattice results for the connected spin averaged amplitudes C_u and C_d at finite quark mass.

κ	m_π/m_ρ	C_u	C_d
0.1560	0.833(5)	1.100(8)	-0.307(3)
0.1565	0.809(15)	1.102(11)	-0.308(4)
0.1570	0.758(11)	1.025(12)	-0.297(8)
0.1575	0.686(11)	1.018(24)	-0.295(10)

equal to the (proton) valence quark mass. We emphasize that the expected linear rise in $R_A^{SUM}(t)$ is manifest for all four quark masses.

The results of the fits to R_A^{SUM} according to Eq. (5) are collected in Table I. We find only a weak dependence on the quark mass. Note that the statistical errors to the connected amplitudes, which have been determined using the jackknife method, are below 5%.

B. Disconnected contributions

The disconnected contributions to the axial vector density matrix element can be analyzed in principle with the global summation method too. It has been pointed out, however, in Ref. [21] that the application of this technique induces large statistical fluctuations. We have therefore chosen a slightly modified procedure, the plateau accumulation method (PAM) [21], which leads to a much better signal to noise ratio. The PAM ratio is defined as

$$R_{A_\mu}^{PAM}(t, \Delta t_0, \Delta t) = \sum_{y_0=\Delta t_0}^{t-\Delta t} R_{A_\mu}^{PLA}(t, y_0), \quad (6)$$

where

$$R_{A_\mu}^{PLA}(t, y_0) = \frac{\sum_{\vec{x}} \left\langle P^\dagger(\vec{0}, 0) \sum_y [\bar{q} \gamma_\mu \gamma_5 q](\vec{y}, y_0) P(\vec{x}, t) \right\rangle}{\sum_x \langle P^\dagger(\vec{0}, 0) P(\vec{x}, t) \rangle} - \left\langle \sum_y [\bar{q} \gamma_\mu \gamma_5 q](\vec{y}, y_0) \right\rangle. \quad (7)$$

Δt and Δt_0 can be varied in the range $1 \leq \Delta t, \Delta t_0 \leq t$ to study the influence of contributions from excited proton states.

The asymptotic time dependence of R_A^{PAM} is given by

$$R_{A_\mu}^{PAM}(t, \Delta t_0, \Delta t) = B + D_{q,\mu}(t - \Delta t - \Delta t_0), \quad (8)$$

where D_q denotes the disconnected contribution to the axial vector amplitude

$$D_{q,\mu} = \langle N | \bar{q} \gamma_\mu \gamma_5 q | N \rangle_{\text{disc}}. \quad (9)$$

The determination of the numerator of Eq. (7) requires the calculation of the correlation of the proton propagator and the axial vector quark loop $L_{A_\mu}(y_0) = \text{Tr}(\bar{q} \gamma_\mu \gamma_5 q)$ at a given timeslice y_0 . $L_A(y_0)$ has been estimated using the spin ex-

plicit stochastic estimator technique [21] with complex Z_2 noise [24] and 100 stochastic estimates per spin component and configuration.

We display in Fig. 3 the signals¹ $R_{A_3}^{PAM}(t)$, with² $\Delta t_0 = \Delta t = 1$, for the symmetric case, where the (proton) valence quark mass and the ‘‘loop’’ quark mass have been set equal to the sea quark mass. Note that the statistical errors are quite large. In particular, for our lightest quark mass, corresponding to $\kappa_{sea} = 0.1575$, the signal is seen to be weak. We emphasize, however, that the slope of R_A^{PAM} appears not to depend strongly on the quark mass. Thus, excluding the result for the lightest quark mass from the analysis would not change the extrapolation to the chiral limit within errors.

A similar behavior is found for the nonsymmetric case, where we have set the ‘‘loop’’ quark mass equal to the strange quark mass [19], while keeping the valence quark mass at the sea quark mass. We show the corresponding signals in Fig. 4 for the heaviest and the lightest quark mass. Within sizeable statistical errors one can identify the expected linear decrease reasonably well.³

In Table II we have collected the raw results for $D_{q,3}$ and $D_{s,3}$ at the different quark masses. Apparently, the disconnected contribution to G_A^1 is definitely less than zero, albeit within statistical errors of the order of 50%.

III. RESULTS

A. Chiral extrapolations

In order to arrive at our lattice estimate for G_A^1 , we have to extrapolate the connected (C_u, C_d) and the disconnected amplitudes (D_q, D_s) to the light quark mass. Since the ‘‘loop’’ quark mass in D_s is kept fixed at the strange quark mass, this quantity serves as a semiquenched estimate for the strange quark contribution to G_A^1 .

We display the (unrenormalized) lattice data and the corresponding fits as a function of the (sea) quark mass in Fig. 5. As mentioned above, the mass dependence of all the amplitudes is weak and the linear ansatz for the extrapolations is in accord with our data. Within errors, D_q and D_s do agree. We conclude that, to the present level of accuracy, flavor symmetry of the disconnected parts appears to be maintained in ($n_f = 2$) full QCD. Note that the disconnected contribution to G_A^1 , given by $2D_q + D_s$, is larger than the connected contribution C_d , suggesting a sizeable modification to the OZI inspired estimate of the singlet coupling.

At the light quark mass, being determined by the requirement that the ratio m_π/m_ρ on the lattice equals the experimental result [19], we find

¹Note that we have used only the combination $\gamma_3 \gamma_5$ in Eq. (7), since we found the signals corresponding to the combinations $\gamma_1 \gamma_5$ and $\gamma_2 \gamma_5$ to be dominated by statistical noise.

²The signals $R_A^{PAM}(t)$ with $\Delta t_0 = \Delta t > 1$ are too noisy to extract a reliable signal.

³The same situation is found at $\kappa_{sea} = 0.1565$. For $\kappa_{sea} = 0.1570$ however, we observed a linear decrease for small t , though the asymptotic behavior is not clear.

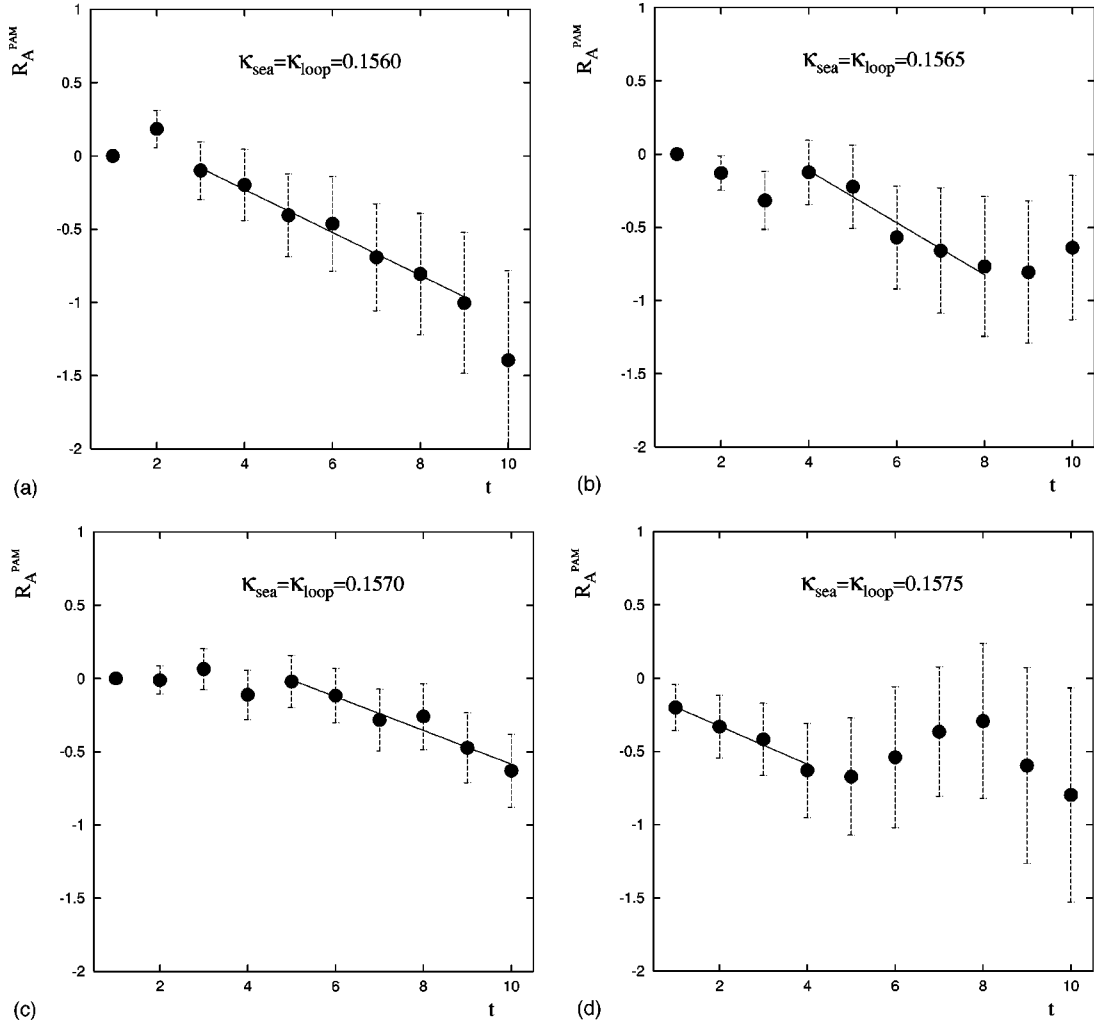


FIG. 3. The ratio $R_{A_3}^{PAM}(t)$ with $\Delta t_0=\Delta t=1$ for the disconnected symmetric amplitudes $D_{q,3}=\langle P(\kappa_{sea})|(\bar{q}\gamma_3\gamma_5q)(\kappa_{sea})|P(\kappa_{sea})\rangle$ at our sea quark masses. The fits (range and value) are indicated by solid lines.

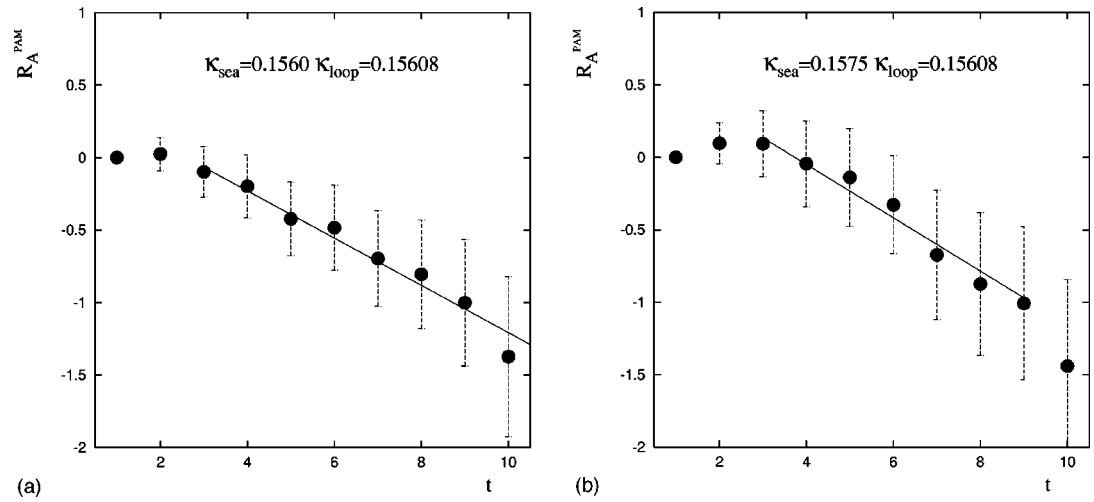


FIG. 4. The ratio $R_{A_3}^{PAM}(t)$ with $\Delta t_0=\Delta t=1$ for the disconnected nonsymmetric amplitudes $D_{s,3}=\langle P(\kappa_{sea})|(\bar{q}\gamma_3\gamma_5q)(\kappa_s)|P(\kappa_{sea})\rangle$ at the heaviest and the lightest sea quark mass, and $\kappa_s=0.15608$. The fits (range and value) are indicated by solid lines.

TABLE II. Lattice results for the disconnected amplitudes $D_{q,3} = \langle P(\kappa) | [\bar{q} \gamma_3 \gamma_5 q](\kappa) | P(\kappa) \rangle_{dis}$ and $D_{s,3} = \langle P(\kappa) | [\bar{q} \gamma_3 \gamma_5 q](\kappa_s) | P(\kappa) \rangle_{dis}$. The value of the hopping parameter $\kappa_s = 0.15608$ corresponds to the strange quark mass [19].

κ	m_π/m_ρ	D_q	D_s
0.1560	0.833(5)	-0.146(60)	-0.163(58)
0.1565	0.809(15)	-0.177(97)	-0.125(74)
0.1570	0.758(11)	-0.119(62)	-0.129(82)
0.1575	0.686(11)	-0.130(69)	-0.184(76)

$$C_u = 0.953(25), \quad C_d = -0.290(11), \quad (10)$$

$$D_q = -0.108(63), \quad D_s = -0.166(91).$$

The numbers in brackets denote the statistical errors, obtained by a jackknife analysis of the extrapolation.

From the appropriate combinations of these amplitudes one can extract the lattice values of the singlet and nonsinglet couplings, as well as the contributions of each single quark flavor to these quantities. The results are collected in Table III. Note that the nonsinglet couplings have been calculated assuming flavor symmetry of the disconnected parts.

B. Renormalization and physics results

In continuum QCD the flavor nonsinglet current A_μ^{NS} is conserved in the chiral limit. Thus it needs no renormalization. The flavor singlet axial vector current A_μ^S on the other hand is not conserved due to the presence of the axial vector anomaly. This leads in the continuum to a nontrivial renormalization of G_A^1 . In second order perturbation theory A_μ^S picks up a logarithmic divergence in the cutoff, which induces a renormalization scale dependence on the axial vector flavor singlet coupling, $G_A^1 = G_A^1(\mu^2)$. The associated anomalous dimension is known to 3 loops [25]. Fortunately, it turns out that the μ^2 dependence of G_A^1 is very weak, e.g., increasing μ^2 from 10 GeV² to infinity decreases the value of G_A^1 by about 10% only; see Ref. [5].

The situation is slightly more involved in the Wilson discretization of lattice QCD [26]. Already the nonsinglet current A_μ^{NS} is not conserved and has to be renormalized by a finite factor Z_A^{NS} . On top of this the singlet current suffers from the axial anomaly. The resulting scale dependence of Z_A^S might be different from the continuum form, as the axial anomaly mixes with the Wilson term.

TABLE III. Lattice results at the light quark mass for the contribution of each quark flavor and for the axial vector couplings of the nucleon. (Z_A^{NS} , Z_A^S denotes the (non)singlet axial vector renormalization constant.

$\Delta u = C_u + D_q$	$\Delta_d = C_d + D_q$	$\Delta_s = D_s$
0.85(10)	-0.398(97)	-0.166(91)
$G_A^1/Z_A^S = C_u + C_d + 2D_q + D_s$ 0.28(16)	$G_A^3/Z_A^{NS} = C_u - C_d$ 1.243(28)	$G_A^8/Z_A^{NS} = C_u + C_d$ 0.663(25)

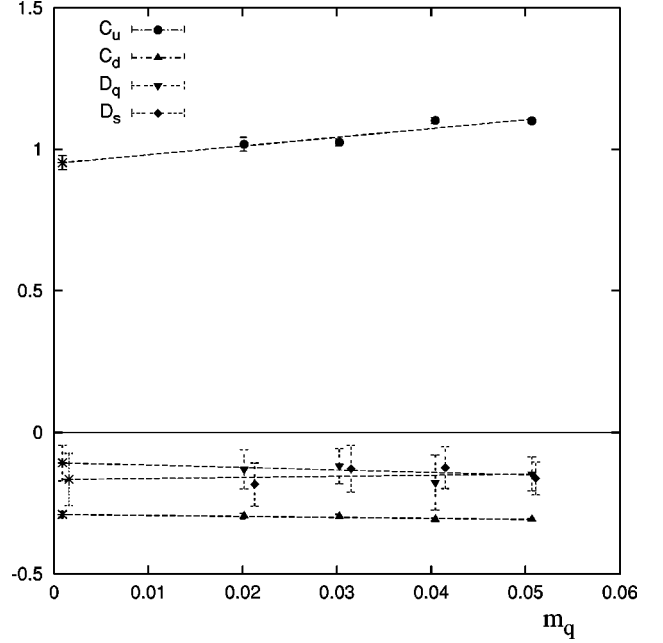


FIG. 5. Extrapolation of the unrenormalized lattice amplitudes to the light quark mass. The fits are indicated by dashed lines, the results of the fits by bursts. To avoid cluttering the data $D_s(m_q)$ have been slightly shifted.

In full QCD both, Z_A^{NS} and Z_A^S , are known only to first order (tadpole improved) lattice perturbation theory [27,28], where they agree. For the nonsinglet current, nonperturbative renormalization procedures have been developed and used in the quenched approximation [29,30]. Those methods, when applied to the case of full QCD, will yield a reliable value for Z_A^{NS} .

The μ^2 dependence of Z_A^S however, which occurs beyond first order, has not been calculated yet. One may hope of course, that it is as weak as in the continuum.

Thus, in view of the current state of analysis, we have used the first order tadpole improved estimate for $Z_A^{NS} = Z_A^S$,

$$Z_A^{NS} = \frac{1}{2\kappa} \left(1 - \frac{3\kappa}{4\kappa_c} \right) \left(1 - 0.31 \alpha_{\overline{MS}} \left(\frac{1}{a} \right) \right), \quad (11)$$

with $\alpha_{\overline{MS}}(1/a) = 0.215$, $\kappa_c = 0.158507$, and $\kappa = \kappa_l = 0.15846$, $\kappa = \kappa_s = 0.15608$ for the light and strange quark insertions, respectively [19].

Unfortunately this choice makes it difficult to determine the scale μ^2 at which we calculate G_A^1 . The renormalized

TABLE IV. Renormalized results at the light quark mass for the contribution of each quark flavor and for the axial vector couplings of the nucleon. For the definitions of the quantities, see Table III.

Δu	Δ_d	Δ_s	G_A^1	G_A^3	G_A^8
0.62(7)	-0.29(6)	-0.12(7)	0.20(12)	0.907(20)	0.484(18)

results are compiled in Table IV. Comparing the estimates for G_A^1 and G_A^8 one finds that the disconnected contributions lead to a violation of the Ellis-Jaffe sum rule by more than 50%, which is consistent with the experimental finding. Note that there is a 30% discrepancy between our estimate of the triplet coupling G_A^3 and the experimental value, $G_A^3 = 1.2670 \pm 0.0035$ [31]. This points to the presence of sizeable higher order or even nonperturbative contributions to Z_A^{NS} . An uncertainty of similar size in Z_A^1 would, however, be well covered by the statistical errors of 50% in G_A^1 .

IV. DISCUSSION AND OUTLOOK

We have calculated connected and disconnected contributions to the flavor singlet axial vector coupling of the proton in a full QCD $n_f=2$ lattice simulation with Wilson fermions. We find G_A^1 , within large uncertainties, to be consistent with the experimental result and with previous quenched estimates. This indicates that the substantial violation of the Ellis-Jaffe sum rule might be caused mainly by the gluonic properties of the vacuum.

The major sources of uncertainty are the large statistical fluctuations of the disconnected parts and the use of the 1st order estimate for Z_A^S .

The statistical quality of disconnected axial vector insertions, achieved with state of the art stochastic estimator methods and with a sample size of 200 configurations, is encouraging but not yet satisfactory. Ideas to improve on this situation are to use larger lattices, where self averaging effects will help, to adapt the stochastic estimator techniques to the axial vector case, e.g., by use of correlated noise and, last but not least, by increased statistics. Work along these lines is in progress.

The nonperturbative determination of Z_A^S presents a major problem. One possible solution is to perform a nonperturbative renormalization of the topological charge and then to use the ‘‘topological method’’ to extract the flavor singlet axial vector renormalization constant.

Having overcome these problems one has to study cutoff and volume dependence of G_A^1 . Finally, as a future project, one should perform full QCD lattice simulations with $n_f \geq 3$ nondegenerate dynamical fermions. This would allow for a realistic estimate of D_s and of the amount of flavor symmetry breaking of the disconnected contributions.

ACKNOWLEDGMENTS

This work has been supported by the DFG grants Schi 257/1-4, 257/3-2, 257/3-3 and by the DFG Graduiertenkolleg ‘‘Feldtheoretische Methoden in der Statistischen und Elementarteilchenphysik.’’ The connected contributions have been computed on the Cray T3E systems of ZAM at FJZ. The disconnected parts were calculated on the APE100 computers at IfH Zeuthen and on the Quadrics machine provided by the DFG to the Schwerpunkt ‘‘Dynamische Fermionen,’’ operated by the University of Bielefeld. We thank the staffs of these institutions for their kind support.

-
- [1] EMC Collaboration, J. Ashman *et al.*, Nucl. Phys. **B328**, 1 (1989); Phys. Lett. B **206**, 364 (1988).
 - [2] SMC Collaboration, B. Adeva *et al.*, Phys. Lett. B **302**, 533 (1993); D. Adams *et al.*, *ibid.* **329**, 399 (1994); D. Adams *et al.*, *ibid.* **339**, 322(E) (1994); D. Adams *et al.*, *ibid.* **357**, 248 (1995); B. Adeva *et al.*, *ibid.* **369**, 93 (1996).
 - [3] SLAC-E142 Collaboration, P.L. Anthony *et al.*, Phys. Rev. Lett. **71**, 959 (1993).
 - [4] SLAC-E143 Collaboration, K. Abe *et al.*, Phys. Rev. Lett. **75**, 25 (1995); **74**, 346 (1995); **76**, 587 (1996).
 - [5] SMC Collaboration, D. Adams *et al.*, Phys. Rev. D **56**, 5330 (1997).
 - [6] SLAC-E154 Collaboration, K. Abe *et al.*, Phys. Lett. B **405**, 180 (1997).
 - [7] J. Ellis and R.L. Jaffe, Phys. Rev. D **9**, 1444 (1974); **10**, 1669 (1974).
 - [8] F.E. Close and R.G. Roberts, Phys. Lett. B **316**, 165 (1993).
 - [9] G. Veneziano, Mod. Phys. Lett. A **4**, 1605 (1989).
 - [10] J.W. Negele, Nucl. Phys. B (Proc. Suppl.) (to be published), hep-lat/9810053.
 - [11] R. Gupta and J.E. Mandula, Phys. Rev. D **50**, 6931 (1994).
 - [12] B. Allés *et al.*, Phys. Lett. B **336**, 248 (1994).
 - [13] R. Altmeyer *et al.*, Nucl. Phys. B (Proc. Suppl.) **34**, 376 (1994).
 - [14] M. Teper, Phys. Lett. B **232**, 227 (1989).
 - [15] A. Di Giacomo and E. Vicari, Phys. Lett. B **275**, 429 (1992).
 - [16] M. Fukugita, Y. Kuramashi, M. Okawa, and A. Ukawa, Phys. Rev. Lett. **75**, 2092 (1995).
 - [17] S.J. Dong, J.F. Lagaë, and K.F. Liu, Phys. Rev. Lett. **75**, 2096 (1995).
 - [18] B. Allés, G. Boyd, M. D’Elia, and A. Di Giacomo, Nucl. Phys. B (Proc. Suppl.) **63**, 239 (1998).
 - [19] SESAM Collaboration, N. Eicker *et al.*, Phys. Rev. D **59**, 014509 (1999).
 - [20] M. Fukugita, Y. Kuramashi, M. Okawa, and A. Ukawa, Phys. Rev. D **51**, 5319 (1995).
 - [21] SESAM Collaboration, S. Güsken *et al.*, Phys. Rev. D **59**, 054504 (1999).
 - [22] L. Maiani, G. Martinelli, M.L. Paciello, and B. Taglienti, Nucl. Phys. **B293**, 420 (1987).
 - [23] S. Güsken, Nucl. Phys. B (Proc. Suppl.) **17**, 361 (1990).
 - [24] S.J. Dong and K.F. Liu, Nucl. Phys. B (Proc. Suppl.) **26**, 353 (1992).
 - [25] S.A. Larin, Phys. Lett. B **334**, 192 (1994); **303**, 113 (1993);

- K.G. Chetyrkin, and J.H. Kühn, Z. Phys. C **60**, 497 (1993).
- [26] L.H. Karsten and J. Smit, Nucl. Phys. **B183**, 103 (1981).
- [27] G.P. Lepage and P.B. Mackenzie, Phys. Rev. D **48**, 2250 (1993); G.P. Lepage, proceedings of the 1996 Schladming School on “Pertubative and Nonpertubative Aspects of Quantum Field Theory,” hep-lat/9607076.
- [28] R. Groot, J. Hoek, and J. Smit, Nucl. Phys. **B237**, 111 (1984).
- [29] S. Capitani *et al.*, Nucl. Phys. B (Proc. Suppl.) **63**, 153 (1998).
- [30] V. Gimenez, L. Giusti, F. Rapuano, and M. Talevi, Nucl. Phys. **B540**, 472 (1999).
- [31] Particle Data Group, C. Caso *et al.*, Eur. Phys. J. C **3**, 1 (1998).